

**Immobilization of Sulfur by Constructing Three-dimensional  
Nitrogen-Rich Carbons for Long Life Lithium-Sulfur Batteries**

Yingbin Tan, Zihui Zheng, Shiting Huang, Yongzhe Wang, Zhonghui Cui, Jianjun  
Liu\* and Xiangxin Guo\*

State Key Laboratory of High Performance Ceramics and Superfine Microstructure,  
Shanghai Institute of Ceramics, Chinese Academy of Sciences, Shanghai 200050,  
China;

Phone and Fax: +86-21-5566 4581.

\*E-mail: [jliu@mail.sic.ac.cn](mailto:jliu@mail.sic.ac.cn), [XXGuo@mail.sic.ac.cn](mailto:XXGuo@mail.sic.ac.cn)

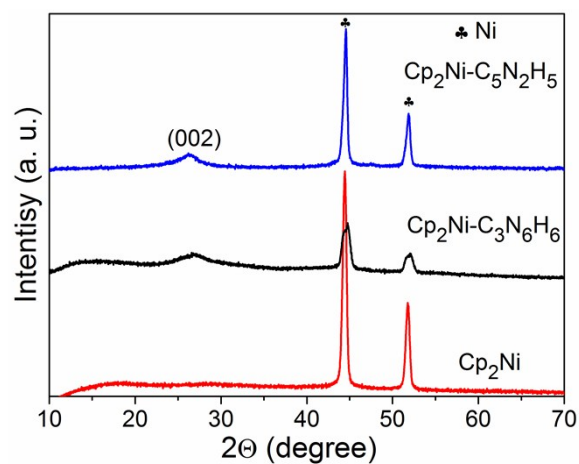


**Fig. S1** Powder XRD patterns of the calcined products by using nickelocene, nickelocene ( $\text{Cp}_2\text{Ni}$ ) and 2-methylimidazole ( $\text{C}_5\text{N}_2\text{H}_5$ ), nickelocene and melamine ( $\text{C}_3\text{N}_6\text{H}_6$ ).

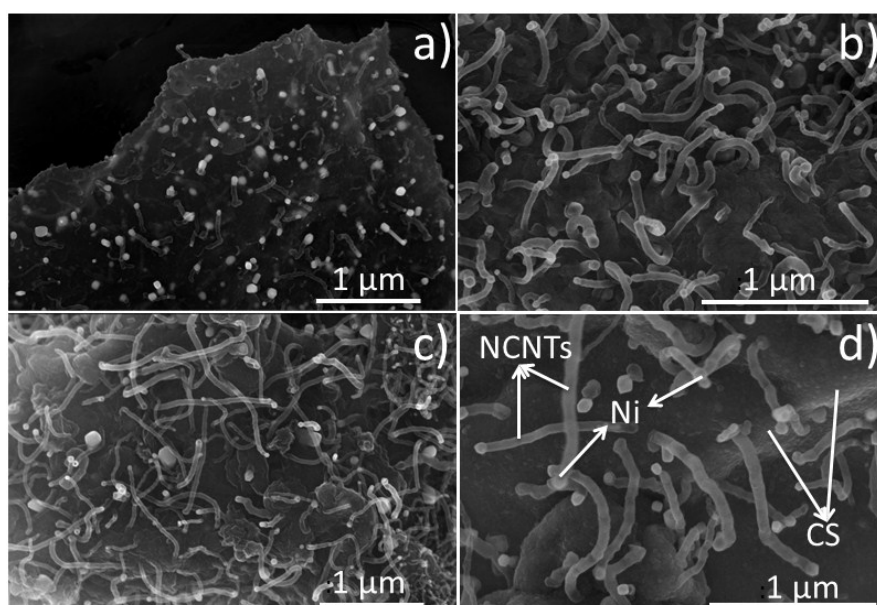


**Fig. S2** SEM images of the obtained Ni@NCNTs-CS by using different mass ratios between nickelocene and melamine: a) 1:2.5, b) 1:5 and c) 1:10. d) SEM images of the obtained NCNTs-CS at Ar- $\text{H}_2$  atmosphere using 1:10 ratios between nickelocene and melamine.

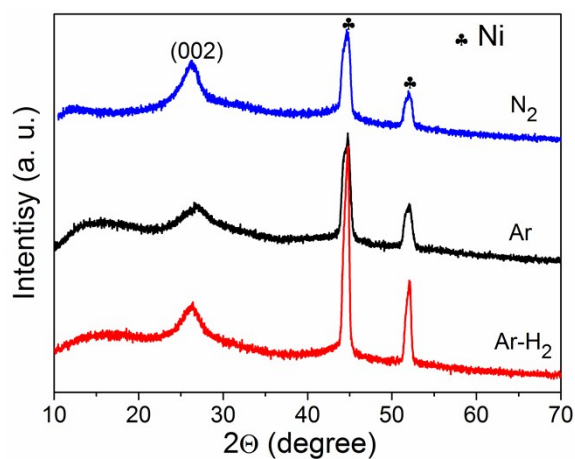


**Fig. S3** Powder XRD patterns of as-prepared Ni@NCNTs-CS at N<sub>2</sub>, Ar and Ar-H<sub>2</sub> atmosphere.

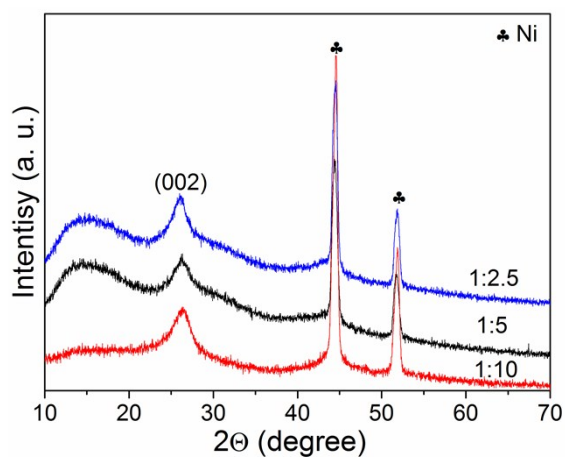


**Fig. S4** Powder XRD patterns of the obtained Ni@NCNTs-CS by using different mass ratios between nickelocene and melamine: 1:2.5, 1:5 and 1:10.

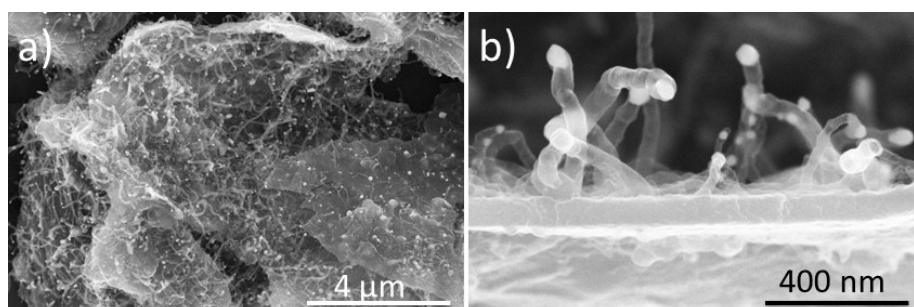


**Fig. S5** SEM images of the obtained Ni@NCNTs-CS at N<sub>2</sub> atmosphere using 1:10 ratios between nickelocene and melamine.

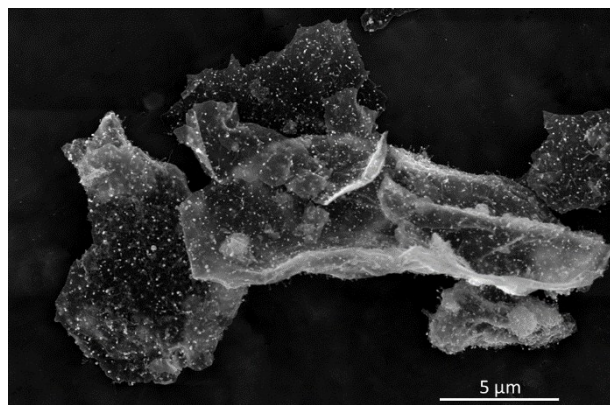


**Fig. S6** SEM images of the obtained Ni@NCNTs-CS at Ar atmosphere using 1:5 ratios between nickelocene and melamine.

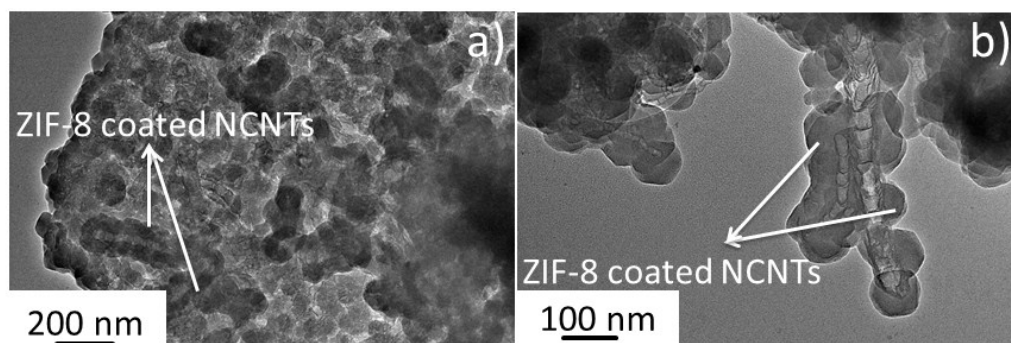


**Fig. S7** TEM images of the obtained NCNTs-CS-ZIF-8 composite.

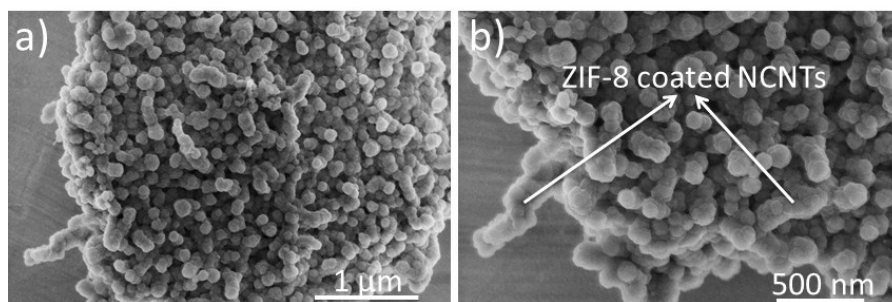


**Fig. S8** SEM images of the obtained NCNTs-CS-ZIF-8 composite.

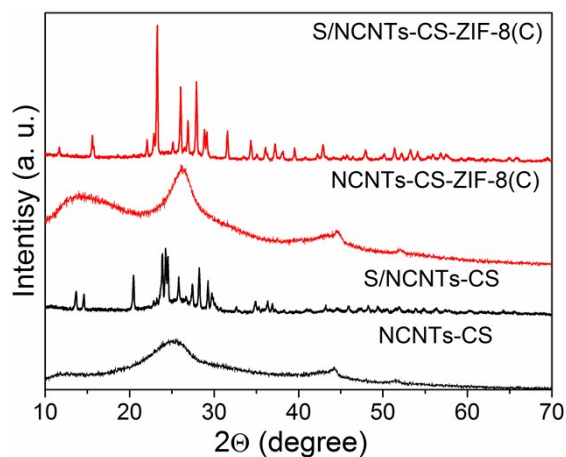


**Fig. S9** Powder XRD patterns of as-prepared NCNTs-CS, ZIF-8, NCNTs-CS-ZIF-8 and NCNTs-CS-ZIF-8(C).

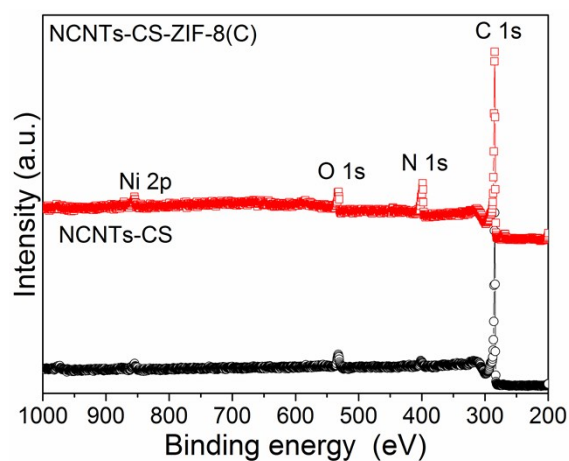


**Fig. S10** XPS spectrum of a) NCNTs-CS and b) NCNTs-CS-ZIF-8(C).

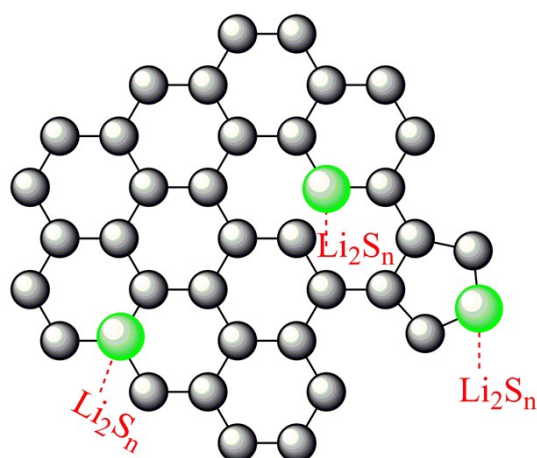


**Fig. S11** The bonding interface between  $\text{Li}_2\text{S}_n$  and nitrogen atom.

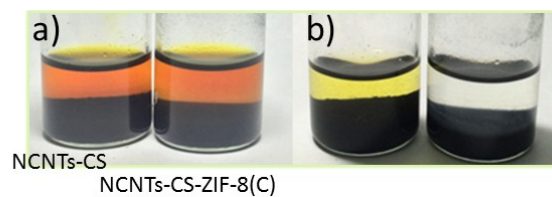


**Fig. S12** Sealed vials of a lithium polysulfides solution ( $\text{Li}_2\text{S}_6$  dissolved in DOL/DME solvents) containing NCNTs-CS and NCNTs-CS-ZIF-8(C) powder: (a) after 0 h, (b) after 0.5 h.

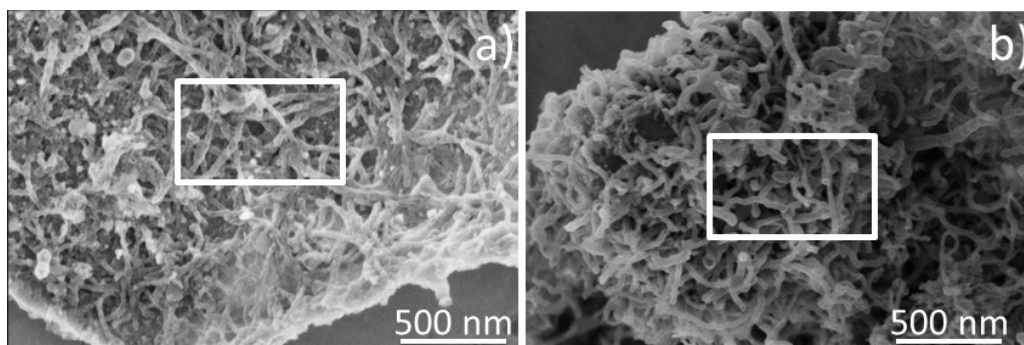


**Fig. S13** SEM images of a) S/NCNTs-CS and b) S/NCNTs-CS-ZIF-8(C).

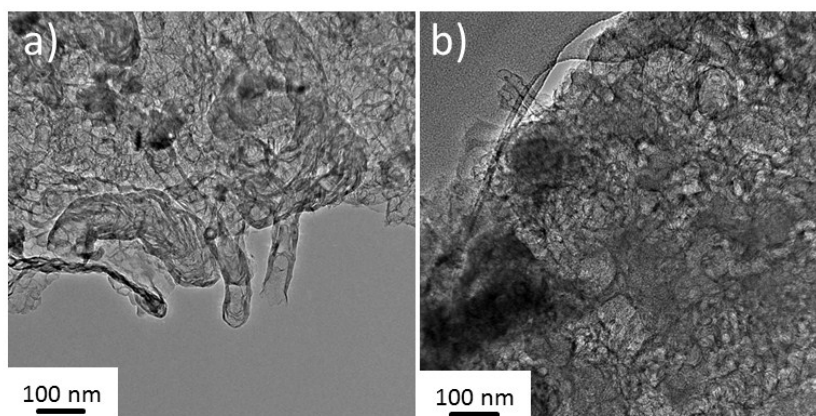


**Fig. S14** TEM images of a) S/NCNTs-CS and b) S/NCNTs-CS-ZIF-8(C).

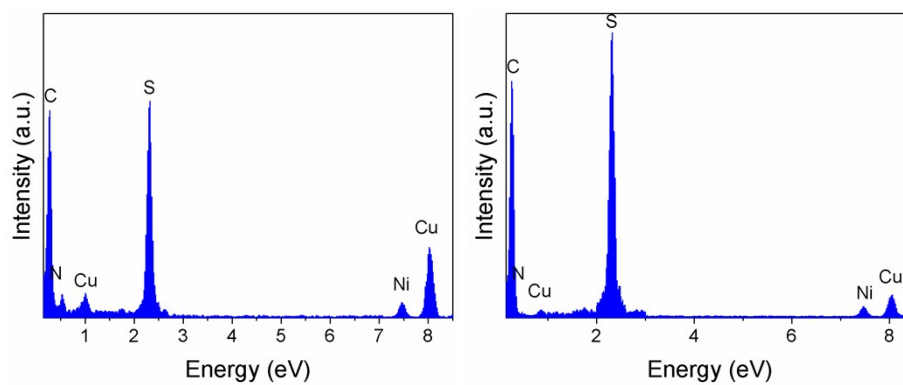


**Fig. S15** EDX spectrum of the area in the white square of **Fig. S13**.

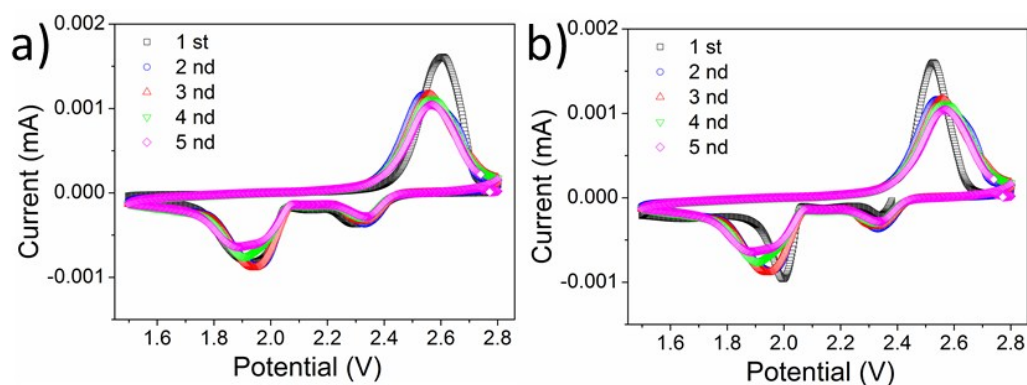


**Fig. S16** CVs of a) S/NCNTs-CS and b) S/NCNTs-CS-ZIF-8(C) in the voltage range of 1.5-2.8 V versus  $\text{Li}^+/\text{Li}$ .

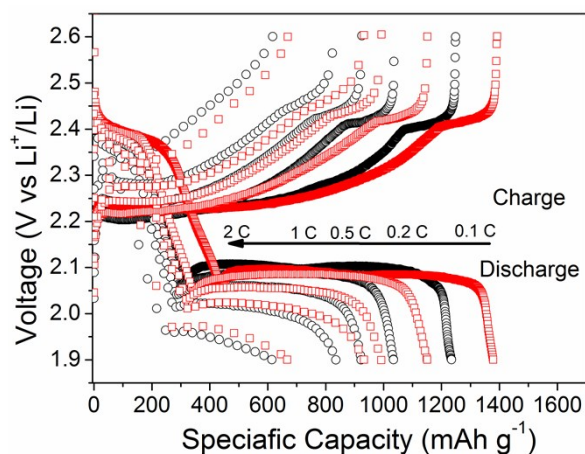


**Fig. S17** The discharge-charge curves of the batteries with the S/NCNTs-CS and S/NCNTs-CS-ZIF-8(C) cathodes at different C rates.

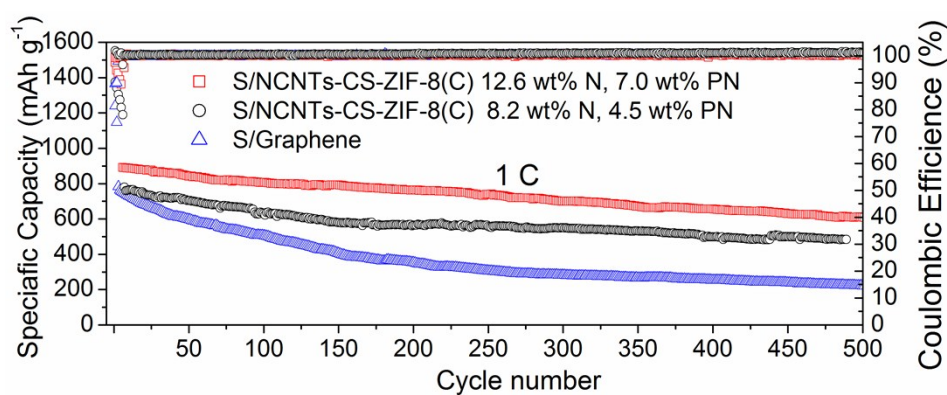


**Fig. S18** The long-term cycling performance and Coulombic efficiencies of S/Graphene and S/NCNTs-CS-ZIF-8(C) with different nitrogen content at 1 C.

**Table S1.** The contents of carbon, nitrogen, oxygen in the resulting NCNTs-CS and NCNTs-CS-ZIF-8(C) via elemental analysis, and the content of nickel in the NCNTs-CS and NCNTs-CS-ZIF-8(C) by ICP measurement.

Samples	C (wt%)	N (wt%)	O (wt%)	Ni (wt%)	graphitic-N (wt %)	pyrrolic-N (wt %)	pyridinic-N (wt %)
NCNTs-CS	85.9	4.5	4.2	5.4	0.4	2.6	1.5
NCNTs-CS- ZIF-8(C)	80.7	12.6	4.5	4.2	1.5	4.1	7.0

It is inferred that these N-doped and O-doped sites in the carbon matrix can produce abundant active sites to promote the surface affinity for polysulfides and lithium sulfides.